

Cont 770304-13

**TITLE:** GROWTH AND SATURATION OF INSTABILITY OF SPHERICAL IMPLOSIONS DRIVEN BY LASER OR CHARGED PARTICLE BEAMS

**AUTHOR(S):** R. L. McCrory, R. L. Morse, and K. A. Taggart

**SUBMITTED TO:** ANS Mathematics and Computation Division  
Topical Meeting, Tucson, Arizona,  
March 27-30, 1977

**NOTICE**  
PORTIONS OF THIS DOCUMENT ARE AVAILABLE. It has been reproduced in whole or in part to permit the broader availability.

**NOTICE**  
This report was prepared as an account of work sponsored by the United States Government. Neither the United States nor the United States Energy Research and Development Administration, nor any of their employees, nor any of their contractors, subcontractors, or their employees, makes any warranty, express or implied, or assumes any legal liability or responsibility for the accuracy, completeness, or usefulness of any information, apparatus, product, or process disclosed, or represents that its use would not infringe privately owned rights.

By acceptance of this article for publication, the publisher recognizes the Government's (license) rights in any copyright and the Government and its authorized representatives have unrestricted right to reproduce in whole or in part said article under any copyright secured by the publisher.

The Los Alamos Scientific Laboratory requests that the publisher identify this article as work performed under the auspices of the USERDA.

  
**Los Alamos**  
**Scientific Laboratory**  
of the University of California  
LOS ALAMOS, NEW MEXICO 87545

An Affirmative Action/Equal Opportunity Employer

**NOTICE**  
PORTIONS OF THIS DOCUMENT ARE AVAILABLE. It has been reproduced in whole or in part to permit the broader availability.

UNITED STATES  
ENERGY RESEARCH AND  
DEVELOPMENT ADMINISTRATION  
CONTRACT W-740-ENG-33

FORM NO. 10  
MAY 1962 EDITION  
GSA GEN. REG. NO. 27



Growth and Saturation of Instability of  
Spherical Implosions Driven by  
Laser or Charged Particle Beams

by

R. L. McCrory  
University of Rochester  
Laboratory for Laser Energetics

R. L. Morse  
University of Arizona  
Department of Nuclear Engineering

K. A. Taggart  
Los Alamos Scientific Laboratory

ABSTRACT

The inertial confinement approach to controlled fusion requires that small thin walled spherical shells of fuel and other materials be imploded, compressed and heated by laser or charged particle beams. In most cases of interest the implosion of such thin shells is unstable to the growth of spherical asymmetries.

We have developed and used two numerical simulation techniques to study these instabilities. The first technique is used to study the small amplitude growth of the instabilities by employing a perturbation method. The derivation of the Hamiltonian model on which the technique is based is developed here. The second technique is a fully non linear two dimensional hydrodynamics and heat flow technique (PAL) which we have used to follow the large amplitude development and saturation of the instabilities. The examples of calculations shown demonstrate the utility of the method and the range of different saturation phenomena which may be expected.

## I. INTRODUCTION

The central idea of inertial confinement controlled fusion is that nuclear fusion fuel can be compressed and heated to economical burning conditions by implosion of pellets containing the fuel. Implosion is caused by ablating material from the surface of a pellet with an external energy input from a focused laser or charged particle beam. Ref. 1 explains in more detail that symmetric spherical implosions, which are most effective for producing economical burning conditions, are made much more effective by the inclusion of thin layers of non fuel material, as well as by making the fuel part of a pellet a thin, hollow, spherical shell. Unfortunately, the performance of such thin shell systems can be greatly reduced by spherical assymetries caused by assymetry of the external heating, or by Rayleigh-Taylor type hydrodynamic instability caused by material acceleration and density gradients. The magnitudes of these phenomena and the contribution of effects which mitigate them, such as thermal conduction and details of density profiles, can be calculated for many cases of interest from a partially linearized numerical treatment of the hydrodynamics and heat flow equations which introduces spherical assymetries as angle dependent perturbations of an exact spherically symmetric treatment. This method, which is more economical than full multi-dimension hydrodynamics, and consequently permits needed parameter studies that would otherwise be almost impossible, is described in section II. The method presented here represents a major improvement over the earlier perturbation method used in Ref. 1. With the new method, which in contrast with that of Ref. 1, is based entirely on a Hamiltonian Model, problems can now be run through collapse of an implosion to the center and at considerably less cost. Results of recent studies with a code called PANSY using this method will be published elsewhere (2).

In those cases where axisymmetric disturbances grow to large amplitudes, particularly as a result of fast growing instabilities whose wavelengths are much less than the spherical shell circumference, a multi dimensional hydrodynamics and heat flow numerical method is needed which is capable of treating the highly distorted flows involved in these particular problems. Section III presents a Particle-In-Cell type method (3) developed for this purpose, which contains more of the features and advantages of Lagrangean methods than the earlier PIC methods while retaining the advantages of fixed grids in handling distorted flows. The method is called PAL for Particle Lagrangean. Section III concludes with an important sample result obtained with this method.

## SECTION II

### A. Unperturbed Model

The Hamiltonian model from which the difference equations for the linear stability method are obtained consists of a nested set of shells which in the absence of perturbations are concentric and have radii  $r_j$ , radial velocities  $v_{rj}$  and surface mass densities,  $M_j$ , per steradian. Thermodynamic properties are defined, i.e., centered, in a homogeneous massless fluid between zones. These properties include pressure and temperature,  $P_j$  and  $T_j$ :  $P_j$  and  $T_j$  are in the region between  $r_{j-1}$  and  $r_j$ . The radial accelerations of the mass are determined directly by the differences between adjacent pressures. The first and last points of the calculation are mass points at  $r_1$  and  $r_{jmax}$ , the former being at the origin, i.e.,  $r_1 = 0$ , if there is no void in the case and at the time in question or at some  $0 < r$ , if there is. The heat flow between the thermodynamic regions,  $F_j$ , energy per steradian per second, then passes through the mass surfaces of area  $A_j = r_j^2$  and is defined there. This description of the unperturbed system is simply a one dimensional, spherical, Lagrangian hydrodynamics and heat flow scheme (Ref. 3). The differential equations of motion of this model are:

$$\begin{aligned} 1) \quad M_j \frac{dv_{rj}}{dt} &= -r_j^2 (P_{j+1} - P_j), \quad (\equiv r_{ro, j}, \text{ see below}) \\ 2) \quad \frac{dr_j}{dt} &= v_{rj} \\ 3) \quad F_j &= \frac{-\kappa_j (T_{j+1} - T_j) r_j^2}{[(r_{j+1} + r_j)/2 - (r_j + r_{j-1})/2]} = \frac{[\kappa(T_{j+1}) + \kappa(T_j)] (T_{j+1} - T_j) r_j^2}{(r_{j+1} - r_j)/2} \end{aligned}$$

We chose to average zone center the thermal conductivity,  $\kappa$ , to zone boundaries. The choice of the radial increment across which the temperature gradient is defined in eq. (3) is the simplest approximately

spatially centered form. It could be improved at some expense in complexity by averaging by volume instead of by length. The  $F_j$ 's are used to advance the thermodynamic state variable, which is specific entropy,  $s_j$ , in our code,

$$4) \quad \frac{ds_j}{dt} = \frac{1}{M_j T_j} \frac{dQ_j}{dt} = \frac{-(F_{j+1} - F_j)}{M_j T_j}$$

and the  $s_j$ 's in turn are used to obtain the  $P_j$ 's from an equation of state

$$5) \quad P_j = P_j(s_j, \rho_j), \text{ where } \rho_j = \frac{3M_j}{(r_j^3 - r_{j-1}^3)}.$$

An analytic ( $\gamma$  law) entropy based procedure is described below (near eq. 82) for both zero and first order variables. If some other state variable such as energy or temperature were used it would also be necessary to integrate an additional energy equation involving the  $PdV/dt$  hydrodynamic work term, where  $V$  is zone volume.

In this code second order accuracy in the time step is obtained in integrating these equations by the use, both in the zero order equations described here and in the first order equations below, by using a modification of the leap frog scheme in which, in units of the time step,  $\Delta t$ , the mass point or surface positions are defined at whole integer times and their velocities at half odd integer times. We need to include some other dependent variables at half and whole time (such as electromagnetic field components when spontaneous magnetic fields are treated later) and to have first order accurate values at half (whole) times which are known to second order only at whole (half) times. Consider then the vectors  $\vec{A}_j$  and  $\vec{B}_j$  of dependent variables for each space index  $j$ , which are to be known to second order in  $\Delta t$  at half and whole times respectively.  $\vec{A}$  and  $\vec{B}$  contain alternate order time derivatives of various dependent variables including  $r$ . These variable vectors, which satisfy the

continuous time differential equations.

$$6a) \quad \frac{d\bar{A}_j}{dt} = \bar{f}_j(\bar{A}, \bar{B})$$

$$6b) \quad \frac{d\bar{B}_j}{dt} = \bar{g}_j(\bar{A}, \bar{B})$$

are then advanced through a full time step,  $\Delta t$ , where  $t = n\Delta t$ , by difference equations of the form.

$$7a) \quad \bar{A}_j^{n+1/2} = \bar{A}_j^{n-1/2} + \Delta t \times \bar{f}_j(\bar{A}_j^n, \bar{B}_j^n)$$

$$7b) \quad \bar{B}_j^{n+1/2} = \bar{B}_j^n + \frac{\Delta t}{2} \times \bar{g}_j(\bar{A}_j^n, \bar{B}_j^n)$$

$$8a) \quad \bar{A}_j^{n+1} = \bar{A}_j^{n+1/2} + \frac{\Delta t}{2} \times \bar{f}_j(\bar{A}_j^{n+1/2}, \bar{B}_j^{n+1/2})$$

$$8b) \quad \bar{B}_j^{n+1} = \bar{B}_j^n + \Delta t \times \bar{g}_j(\bar{A}_j^{n+1/2}, \bar{B}_j^{n+1/2})$$

where the superscripts indicate time and the subscripts are absent from the arguments of  $\bar{f}$  and  $\bar{g}$  because the continuous form in space in general involves spatial derivatives such as  $\bar{\nabla}P$ , and, therefore the spatially differenced forms at index  $j$  will contain non-local values at least from  $j+1$ . While eqs. 7b and 8a are not time centered and are, therefore, only first order accurate in  $\Delta t$ , in all applications it is easily shown that the results are multiplied by another factor of  $\Delta t$  before being added to a second order quantity and, therefore, second order accuracy in  $\Delta t$  is maintained.

### B. Perturbation Treatment

The perturbation treatment consists of calculating first order corrections, which depend on all three dimensions, i.e., on angle variables as well as on radius, to all of the zero order independent variables, which depend only on radius. The inclusion of the required continuous dependence on angle variables is accomplished by using a model which is essentially a three dimensional lagrangian treatment of a spherical system in which the radial zone dimensions remain

finite while the angular (about the spherical center) zone dimensions go to zero. The angular dependence therefore becomes continuous, as indicated in Fig. 1, which shows a cross section through the spherical center, and the point inertial masses at the zone boundary intersections become continuous spherical (to zero<sup>th</sup> order) mass shells. Corresponding to the continuous angular zoning, every point on the mass shells has a three dimensional first order displacement,  $\bar{\xi}$ , which consists of a radial displacement,  $\xi_r$ , and two angular displacements,  $\bar{\xi}_\Omega \equiv r\bar{\Omega}$ , and corresponding first order velocities,  $v_{r1}$  and  $\dot{\bar{\Omega}}$ . Then the equation of motion of a point on the j<sup>th</sup> mass shell, in terms of the linear and angular momenta,  $p_r$  and  $\bar{p}_\Omega$ , is

$$9) \quad \frac{dp_{rj}}{dt} = f_{rj}, \quad \frac{dr_j}{dt} = \frac{p_{rj}}{M_j}$$

$$10) \quad \frac{d\bar{p}_{\Omega j}}{dt} = r_j \bar{f}_{\Omega j}, \quad \frac{d\bar{\Omega}_j}{dt} = \frac{p_{\Omega j}}{M_j r_j^2}$$

where  $\bar{f}$  is the force on the mass,  $M_j$ , subtended by one steradian on the unperturbed mass shell at the  $\bar{\Omega}$  in question, and  $p_{rj} = M_j v_{rj}$ ,  $\bar{p}_{\Omega j} = M_j r_j^2 \dot{\bar{\Omega}}_j$ . After expanding to first order in  $\bar{\xi}$ , equation (9) contains a zero order part which is equivalent to eqs. (1) and (2) above and a first order part of the same form,

$$9a) \quad \frac{dp_{r1}}{dt} = f_{r1j}, \quad \frac{d\xi_{r1}}{dt} = \frac{p_{r1j}}{M_j}$$

Eq. (10) is only first order since we exclude zero<sup>th</sup> order angular motions. To first order in  $\bar{\xi}$ ,  $f_{r1}$  is

$$11a) \quad f_{r1} = -\delta[\Lambda_j^2 (P_{1,j+1} - P_{1,j})] = -[\Lambda_{1j} (P_{0,j+1} - P_{0,j}) + \Lambda_{0j} (P_{1,j+1} - P_{1,j})]$$

Here 0 and 1 subscripts indicate zero<sup>th</sup> and first order quantities respectively, the prefix  $\delta$  indicates the first order part of what follows, and  $\Lambda_j$  is the area of that part of the surface which subtends one



steradian on the unperturbed mass shell ( $A_{o,j} = r_j^2$ ). The exception to the order notation is  $\bar{\xi}$  which is purely first order and so does not carry a 1 subscript. Both  $\xi_r$  and  $\bar{\xi}_\Omega$  contribute to the changes  $\Delta_{1j}$  in the surface area,  $A_j$ , of an element of a mass shell. It is

$$12) \quad \Delta_{1j} \equiv \Lambda_{oj} \left( \frac{2\xi_r}{r} + \bar{\nabla}_\Omega \cdot \bar{\xi}_\Omega \right)_j = \Lambda_{oj} \left( \frac{2\xi_r}{r} + \frac{\partial \bar{\xi}_\Omega}{\partial \bar{\Omega}} \right)_j,$$

where  $\bar{\nabla}_\Omega$  is the gradient with respect to angle variable only, and, therefore, that

$$13) \quad f_{r1} = -r_j^2 \left[ \left( \frac{2\xi_r}{r_j} + \frac{\partial \bar{\xi}_\Omega}{\partial \bar{\Omega}} \right)_j (P_{o,j+1} - P_{o,j}) + (P_{1,j+1} - P_{1,j}) \right]$$

The angular force per steradian,  $\bar{f}_{\Omega 1}$ , has two qualitatively different contributions, i.e.,

$$11b) \quad \bar{f}_{\Omega 1} = {}^1\bar{f}_{\Omega 1} + {}^2\bar{f}_{\Omega 1}.$$

${}^1\bar{f}_{\Omega 1}$  can be thought of as the angular contribution from rotating  $f_{r0}$  away from purely radial by any tip of the  $j^{\text{th}}$  mass surface, and

${}^2\bar{f}_{\Omega 1}$  is caused by angular gradients of the pressure.

It is clear from Fig. 1b that

$$14) \quad {}^1\bar{f}_{\Omega 1} = \frac{-f_{r0}}{r} \frac{\partial \xi_r}{\partial \bar{\Omega}},$$

where  $f_{r0,j} \equiv -r_j^2 (P_{o,j+1} - P_{o,j})$ .

A weighted sum of  ${}^2\bar{f}_{\Omega 1,j \pm 1}$  values is applied to the mass surface along with  $f_{r1}$  as indicated in Fig. 1b. These averaged  ${}^2\bar{f}_{\Omega 1}$  forces resulting from pressure gradients in the angular directions are transferred to the mass shells, which contain the inertial mass, by the rigid, massless radial zone boundary panels. This is a consistent model in spite of the fact that the separation of these panels is taken to be vanishingly small.

Because of the spherical geometry, the contribution from a given angular gradient of  $P_{1,j}$  to  ${}^2\bar{f}_{1,j}$  is greater than to  ${}^2\bar{f}_{1,j-1}$ . This can be derived by integrating the force into the page, Fig. 1c, on supports at  $r_1$  and  $r_2$  caused by a pressure  $P$  applied to a panel between two radii. The forces on supports at  $r_1$  and  $r_2$ , per radian in the plane are

$$15) \quad F_1 = \int_{r_1}^{r_2} df_1 = \int_{r_1}^{r_2} \frac{dr_{j-1}(r_2-r)}{(r_2-r_1)} = \frac{P}{6} [r_2^2 + r_2 r_1 - 2r_1^2]$$

$$16) \quad F = F_{\text{total}} - F = \frac{P(r_2^2 - r_1^2)}{2} - F_1 = \frac{P}{6} [2r_2^2 - r_2 r_1 - r_1^2].$$

Then clearly, since the force on a panel per unit area per unit angle along the direction of the pressure gradient is  $-\partial P/\partial \Omega$ , adding forces at  $r_j$  from the panels between  $r_{j-1}$  and  $r_j$ , and between  $r_j$  and  $r_{j+1}$  gives

$$17) \quad {}^2\bar{f}_{\Omega,j} = -\frac{1}{6} \left\{ \frac{\partial P_{1,j+1}}{\partial \Omega} [r_{j+1}^2 + r_{j+1} r_j - 2r_j^2] + \frac{\partial P_{1,j}}{\partial \Omega} [2r_j^2 - r_j r_{j-1} - r_{j-1}^2] \right\}.$$

The angular vector equations can now be converted into scalar equations by taking angular divergences, i.e., by operating with  $\frac{\partial}{\partial \Omega}$  on the vector equations. This, however, will not be possible when these equations are generalized to include spontaneously generated magnetic fields and off diagonal viscous stress tensor elements. Then instead, vector quantities (actually vector spherical harmonics instead of scalar spherical harmonics---see below) must be employed. Combining eqs. (10), (11b), (14), and (17) and operating with  $\frac{\partial}{\partial \Omega}$  on both sides gives

$$18) \quad \frac{d}{dt} \left( \frac{\partial \tilde{L}_{1,j}}{\partial \dot{z}} \right) = \dot{z}_j \left\{ \left( \frac{\partial}{\partial z} \cdot \frac{\partial}{\partial \dot{z}} \right) (v_{0,i} - v_{0,j}) r_j \right. \\ \left. - \frac{1}{6} \left[ \left( \frac{\partial}{\partial z} \cdot \frac{\partial p_{1,i}}{\partial \dot{z}} \right) \left( r_{j+1}^2 - r_{j-1}^2 - 2r_j^2 \right) + \left( \frac{\partial}{\partial z} \cdot \frac{\partial p_{1,j}}{\partial \dot{z}} \right) \left( 2r_j^2 - r_j r_{j+1} - r_j r_{j-1} \right) \right] \right\}$$

$$19) \quad \frac{d}{dt} \left( \frac{\partial \tilde{L}_{1,j}}{\partial \dot{\theta}} \right) = \dot{\theta}_j r_j^2 \left( \frac{\partial \tilde{L}_{1,j}}{\partial z} \right)$$

The first order hydrodynamic system is completed by substituting eq. (11) into eq. (9) and for this purpose perturbed densities,  $\rho_{1,j}$ , are needed to obtain the perturbed pressures,  $p_{1,j}$ , from derivatives of the equation of state. Suppose a spot on the mass shell at  $r_j$  is small enough that  $(\tilde{V}_{1\Omega} \cdot \tilde{t}_{r,j}) = \partial/\partial z \cdot \tilde{t}_1$  can be taken as uniform over its surface. The change in volume,  $V$ , of the region defined by this spot, the one on the surface at  $r_{j-1}$  subtended by the same unperturbed radii, and straight lines connecting corresponding unperturbed points, has contributions from  $\tilde{t}_{r,j}$  and  $\tilde{t}_{r,j-1}$  and  $\tilde{t}_{z,j}$  and  $\tilde{t}_{z,j-1}$ :

$$20) \quad V_{1j} = V_{1rj} + V_{1\Omega j}$$

$V_{1rj}$  is the volume swept out by the perturbed rotation of the end caps and is

$$21) \quad V_{1rj} = A_j \tilde{t}_{r,j} - A_{j-1} \tilde{t}_{r,j-1}$$

The  $V_{1\Omega j}$  contribution is obtained from integrating the perturbed cross sectional area,  $A_1$  (see eq. 12), of the volume element between mass surfaces. From  $A_{1\Omega}$  at an arbitrary radius,  $r$ , between  $r_{j-1}$  and  $r_j$ ,

$$22) \quad A_{1\Omega} = A_{1\Omega,j} \frac{r}{r_j} \left( \frac{r-r_{j-1}}{r_j-r_{j-1}} \right) + A_{1\Omega,j-1} \left( \frac{r_j-r}{r_j-r_{j-1}} \right) \frac{r}{r_{j-1}}$$

integrating over  $r$  from  $r_{j-1}$  to  $r_j$  gives

$$23) \quad V_{1\Omega_j} = \frac{1}{6} \left[ \frac{A_{1\Omega,j}}{r_j} (2r_j^2 - r_j r_{j-1} - r_{j-1}^2) + \frac{A_{1\Omega,j-1}}{r_{j-1}} (r_j^2 + r_j r_{j-1} - 2r_{j-1}^2) \right]$$

Equations (21) and (23) can be simplified with the relationships between the unperturbed volumes and areas

$$24) \quad \frac{A_{o,j-1}}{A_{o,j}} = \left( \frac{r_{j-1}}{r_j} \right)^2 \quad \text{and} \quad V_{oj} = \frac{(A_j r_j - A_{j-1} r_{j-1})}{3} = \frac{A_{oj} r_j}{3} \left[ 1 - \left( \frac{r_{j-1}}{r_j} \right)^3 \right]$$

and with  $A_{1\Omega,j} = A_{oj} \bar{V}_{\Omega} \cdot \bar{\xi}_{\Omega,j}$  from eq. (12).

Then the desired expression for  $\rho_{1j}$  becomes

$$\begin{aligned} 25) \quad \rho_{1j} &= \frac{-\rho_{oj} V_{1j}}{V_{oj}} \\ &= \frac{-3\rho_{oj}}{\left[ 1 - \left( \frac{r_{j-1}}{r_j} \right)^3 \right]} \left\{ \left[ \frac{\xi_{r,j}}{r_j} - \left( \frac{r_{j-1}}{r_j} \right)^3 \frac{\xi_{r,j-1}}{r_{j-1}} \right] + \right. \\ &\quad \left. + \frac{1}{6} \left[ \frac{\bar{V}_{\Omega} \cdot \bar{\xi}_{\Omega,j}}{r_j^2} (2r_j^2 - r_j r_{j-1} - r_{j-1}^2) + \right. \right. \\ &\quad \left. \left. + \frac{\bar{V}_{\Omega} \cdot \bar{\xi}_{\Omega,j-1}}{r_{j-1}^2} \left( \frac{r_{j-1}}{r_j} \right)^3 (r_j^2 + r_j r_{j-1} - 2r_{j-1}^2) \right] \right\} \\ &= \frac{-3\rho_{oj}}{\left[ r_j^3 - r_{j-1}^3 \right]} \left[ r_j^2 \xi_{r,j} - r_{j-1}^2 \xi_{r,j-1} \right] + \\ &\quad + \frac{1}{6} \left[ r_j \bar{V}_{\Omega} \cdot \bar{\xi}_{\Omega,j} (2r_j^2 - r_j r_{j-1} - r_{j-1}^2) + r_{j-1} \bar{V}_{\Omega} \cdot \bar{\xi}_{\Omega,j-1} (r_j^2 + \right. \\ &\quad \left. + r_j r_{j-1} - 2r_{j-1}^2) \right] \end{aligned}$$

### Spherical Harmonic Expansion

At this point the first order hydrodynamic equations can be expanded in scalar spherical harmonics. This is accomplished by first expanding all scalar quantities such as  $p_1$ ,  $T_1$ ,  $\xi_r$ ,  $(\bar{V}_{\Omega} \cdot \bar{\xi}_{\Omega})$  and  $(\frac{\partial}{\partial t})$  in the form

$$26) \quad P_{1j}(\bar{\Omega}) = \sum_{\ell, m} P_{1j\ell m} Y_{\ell m}(\bar{\Omega}).$$

The  $Y_{\ell m}$ 's may be thought of as orthonormal over  $4\pi$  steradians although their normalization is not important here. The only additional property we require here is the identity

$$27) \quad r^2 \nabla_{\bar{\Omega}}^2 Y_{\ell m}(\bar{\Omega}) = \frac{\partial}{\partial \bar{\Omega}} \cdot \frac{\partial}{\partial \bar{\Omega}} Y_{\ell m}(\bar{\Omega}) = -\ell(\ell+1) Y_{\ell m}(\bar{\Omega}).$$

When expansions of the form of eq. (26) are substituted in all of the equations of motion and the auxiliary relations such as (25), and use is made of eq. (27), it is seen that because of the orthogonality of the  $Y_{\ell m}$ 's the equations separate completely with respect to  $\ell$ , and that the equations for a given  $\ell$  are independent of (i.e., degenerate with respect to)  $m$ . In particular, from eq. (27), the quantities appearing on the right side of the expansion of eq. (18) become

$$28) \quad \frac{\partial}{\partial \bar{\Omega}} \cdot \frac{\partial}{\partial \bar{\Omega}} P_{1j\ell m} Y_{\ell m}(\bar{\Omega}) = -\ell(\ell+1) P_{1j\ell m} Y_{\ell m}(\bar{\Omega})$$

$$\frac{\partial}{\partial \bar{\Omega}} \cdot \frac{\partial}{\partial \bar{\Omega}} \xi_{rj\ell m} Y_{\ell m}(\bar{\Omega}) = -\ell(\ell+1) \xi_{rj\ell m} Y_{\ell m}(\bar{\Omega}).$$

From here on we suppress the subscripts  $\ell$  and  $m$  on dependent variables.

If for simplicity we make the definitions:

$$29) \quad A_j \equiv P_{r1j} = M_j \dot{\xi}_{rj} \quad (\text{using } A_j \text{ for area also should cause no trouble})$$

$$B_j \equiv \xi_r$$

$$C_j \equiv \frac{\partial}{\partial \bar{\Omega}} \cdot \bar{A}_{1j}$$

$$D_j \equiv \frac{\partial}{\partial \bar{\Omega}} \cdot \bar{\Omega}_{1j}$$

then the equations of motion, which are combinations of equations

(9), (10), (13), (18), and (19), become

$$30) \quad \frac{dA_j}{dt} = -r_j^2 \left[ \left( \frac{2B_j}{r_j} + D_j \right) (P_{\sigma, j+1} - P_{\sigma, j}) + (P_{1, j+1} - P_{1, j}) \right]$$

$$31) \frac{dB_j}{dt} = \frac{A_j}{M_j}$$

$$32) \frac{dC_j}{dt} = -\ell(\ell+1)r_j \left\{ B_j r_j (P_{0,j+1} - P_{0,j}) - \frac{1}{6} \left[ P_{1,j+1} (r_{j+1}^2 - r_j^2 - 2r_j^2) + P_{1,j} (2r_j^2 - r_j r_{j-1} - r_{j-1}^2) \right] \right\}$$

$$33) \frac{dD_j}{dt} = \frac{C_j}{M_j r_j^2}$$

In addition an equation of state is required

$$34) P_{1,j} = P_{1,j}(s_{1,j}, \rho_{1,j})$$

and the relationship (25) for  $\rho_{1,j}$  which now reads

$$35) \rho_{1,j} = \frac{3\rho_{0,j}}{(r_j^3 - r_{j-1}^3)} \left\{ \left[ r_j^2 B_j - r_{j-1}^2 B_{j-1} \right] + \frac{1}{6} \left[ r_j D_j (2r_j^2 - r_j r_{j-1} - r_{j-1}^2) + r_{j-1} D_{j-1} (r_j^2 + r_j r_{j-1} - 2r_{j-1}^2) \right] \right\}$$

#### Special Treatment of the Origin

The origin in  $\ell = 1$  calculations is a special case and must be treated in a special way. This fact, which may be intuitively obvious to readers who are familiar with stability analysis, can be understood in the following way, which brings in some concepts needed in the mathematical treatment.

The origin in our treatment of the spatial differencing is a point mass. It could have been a point where thermodynamic variables are centered instead. However, this would not fit in with problems which start with a spherical void in the middle of a system and collapse the first mass surface to a point when material first reaches the center, and we do such problems. Then, since the

origin is a point it can only have a single vector displacement,  $\bar{\xi}_1$ , not a continuous  $\xi_r(\bar{\Omega})$  or  $\bar{\xi}_\Omega(\bar{\Omega})$ . That such a rigid displacement of the origin is only consistent with an  $\ell - 1$  perturbation is perhaps obvious, but we proceed as if it weren't.

Consider now the change in volume of the conical region with straight sides between the origin and the perimeter of a small area,  $A$ ; on the first spherical or almost spherical mass surface outside of the origin, which is at mean radius  $r_2$ . The volume,  $V_{0,2}$ , of this region (see Fig. 1d) is easily seen to be

$$36) \quad V_{0,2} = \frac{A_2 r_2}{3}.$$

If the mass surface is kept fixed and the origin is displaced by  $\bar{\xi}_1$ , the change in volume is then seen to be

$$37) \quad V_{1,2}(\bar{\Omega}) = \frac{-A_2 \bar{\xi}_1 \cdot \bar{r}_2}{3r_2}$$

where  $\bar{r}_2$  is directed to the centroid of  $A$ . If  $\bar{\Omega}$  is a unit vector in the direction of  $r_2$ , then we write

$$38) \quad V_{1,2}(\bar{\Omega}) = \frac{-A_2 \bar{\xi}_1 \cdot \bar{\Omega}}{3}$$

The first order density change caused by motion of the origin is then

$$39a) \quad \rho_{1,2}(\bar{\Omega}) = \frac{-\rho_{0,2} V_{1,2}(\bar{\Omega})}{V_{0,2}} = \frac{\rho_{0,2} (\bar{\xi}_1 \cdot \bar{\Omega})}{r_2}$$

and the total  $\rho_{1,2}$ , including contributions from first order

displacements at  $r_2$  (see eq. 25) is

$$39b) \quad \rho_{1,2}(\bar{\Omega}) = \frac{\rho_{0,2} (\bar{\xi}_1 \cdot \bar{\Omega})}{r_2} + \frac{\rho_{0,2}}{r_2^2} \left[ r_2^2 \xi_{r,2}(\bar{\Omega}) + \frac{r_2^3 (\nabla_{\bar{\Omega}} \cdot \xi_{\Omega,2})}{3} \right]$$

The first order pressure is then

$$40) \quad P_{1,2}(\bar{\Omega}) = \rho_{1,2}(\bar{\Omega}) \left( \frac{\partial p}{\partial \rho} \right)_{j=2}$$

where the pressure derivative, which is of course a zero order quantity,

is calculated at the  $j = 2$  zero order state conditions from whatever equation of state is used.

From eq. (40) and the addition theorem for spherical harmonics it can be seen that  $P_{1,2}(\bar{\Omega})$  can only consist of  $l = 1$  terms; which justifies treating the origin in this special way only for  $l = 1$ .

The theorem when applied to  $l = 1$  states that if  $\theta$  is the angle between  $\bar{\Omega}$  and  $\bar{\Omega}_{\xi_1}$ , then

$$(41) \quad \cos \theta = \frac{4\pi}{3} \sum_{m=-1}^{+1} Y_{1m}(\bar{\Omega}) Y_{1m}(\bar{\Omega}_{\xi_1}).$$

If  $\bar{\Omega}_{\xi_1}$  is the direction of  $\bar{\xi}_1$ , then  $\bar{\xi}_1 \cdot \bar{\Omega} = \xi_1 \cos \theta$  and equation (41) shows that the  $\bar{\Omega}$  dependence of  $\bar{\xi}_1 \cdot \bar{\Omega}$ , and therefore  $P_{1,2}$  from eq. (39), has only the  $l = 1$  form.

In order to obtain the time dependence of  $\bar{\xi}_1$ , and therefore  $P_{1,2}$ , we now need an equation of motion which gives the time dependence of  $\bar{\xi}_1 \cdot \bar{\Omega}$  from  $P_{1,2}(\bar{\Omega})$ , i.e., an equation of the form  $\frac{d}{dt} \bar{\xi}_1 \cdot \bar{\Omega} = P_{1,2}(\bar{\Omega})$ . We start from eqs. (13), (14), and (17) for the forces on a mass shell and take the limit that the radius of the shell in question,  $j = 1$ , goes to zero. If it can be assumed that  $r \xi_x$  and  $r^2 (\nabla_{\bar{\Omega}} \cdot \bar{\xi}_x)$  tend to zero as  $r \rightarrow 0$ , which is true for cases of interest, then eq. (13) gives  $f_{r1} = 0$  for  $r_j = 0$ . Similarly in eq. (14), since  $f_{r0} \sim r^2$ , if  $r \xi_{r1} \rightarrow 0$  as  $r_1 \rightarrow 0$ , then  $f_{\Omega,1} \rightarrow 0$ . Equation (17), however, gives a non-zero contribution. For  $j = 1$ , the second term is zero because there is no  $P_{1,1}$  (which would by our spatial centering convention be inside the origin). The first term gives,

$$(42) \quad f_{\Omega,1}(\bar{\Omega}) = \frac{-r_1^2}{6} \frac{\partial P_{1,2}(\bar{\Omega})}{\partial \bar{\Omega}}$$

The scalar product of the integral of this force over all angles with the unit vector  $\bar{\Omega}$  is



$$(43) \quad \bar{\Omega} \cdot \bar{F}_{1,1} = \int d\Omega r_0^2 \bar{F}_{\Omega_{1,1}}(\bar{\Omega}) = \dots = \frac{r_2^2}{6} \int d\Omega r_0^2 \frac{\partial P_{1,2}(\bar{\Omega})}{\partial \bar{\Omega}}$$

It can be shown that for an arbitrary vector  $\bar{V}_\Omega$  that lies in the surface of a sphere of radius  $r$ , the scalar product of an arbitrary unit vector,  $\bar{\Omega}$ , with the integral,  $\bar{V}_{\Omega_0}$ , of this vector over the sphere is

$$(44) \quad \bar{\Omega} \cdot \bar{V}_{\Omega_0} = \frac{-\alpha r}{3} Y_{1m}(\bar{\Omega})$$

if  $\bar{V}_\Omega$  is such that

$$(45) \quad \bar{V}_\Omega \cdot \bar{V}_\Omega = \alpha Y_{1m}(\bar{\Omega}).$$

If we assume  $P_{1,2}(\bar{\Omega}) \sim Y_{1m}(\bar{\Omega})$  for any particular  $m$  in lieu of expanding in  $Y_{\ell m}$ 's, then since

$$(46) \quad \left[ \bar{V}_\Omega \cdot \frac{\partial P_{1,2}(\bar{\Omega})}{\partial \bar{\Omega}} \right]_{r=r_2} = \frac{1}{r_2} \frac{\partial}{\partial \bar{\Omega}} \cdot \frac{\partial P_{1,2}(\bar{\Omega})}{\partial \bar{\Omega}} = \frac{-\ell(\ell+1)P_{1,2}(\bar{\Omega})}{r_2} = \frac{-2P_{1,2}(\bar{\Omega})}{r_2}$$

because  $\ell=1$ , we have from substituting eqs. (44), (45) and (46) into eq. (43),

$$(47) \quad \bar{\Omega} \cdot \bar{F}_{1,1} = -\frac{r_2^2}{6} \left[ \dots \left( \frac{-P_{1,2}(\bar{\Omega})}{r_2} \right) \left( \frac{r_2}{3} \right) \right] = \dots = \frac{r_2^2 P_{1,2}}{9}$$

(remember this acts on all  $4\pi N_1$ , not just  $N_1$ ).

If the mass per steradian of the mass shell bounding a central void is  $N_1$ , then the mass of the origin mass point when this shell is collapsed is  $4\pi N_1$  and the equation of motion is

$$(48) \quad 4\pi N_1 \frac{d^2 \bar{\xi}_1}{dt^2} = \bar{F}_{1,1}$$

or

$$(49) \quad 4\pi N_1 \frac{d^2}{dt^2} (\bar{\Omega} \cdot \bar{\xi}_1) = \bar{\Omega} \cdot \bar{F}_{1,1} = \dots = \frac{r_2^2 P_{1,2}(\bar{\Omega})}{9}$$

Substituting into eq. (49) from eq. (40) for  $P_{1,2}(\bar{\Omega})$  gives

$$(50) \quad 4\pi N_1 \frac{d^2}{dt^2} (\bar{\Omega} \cdot \bar{\xi}_1) = \dots = \frac{r_2^2 \rho_1}{9} \cdot \left( \frac{\partial \rho}{\partial \rho} \right)_{\bar{\Omega}}$$

In practice we solve this equation by substituting into eq. (39) for  $\rho_{1,2}(\bar{\Omega})$  then into the equation of state for  $P_{1,2}$ , and then substituting into eq. (50). To be consistent with eqs. (39) through (33) we set  $C_1 = D_1 = 0$  and define

$$51) \quad A_1 \equiv \frac{d}{dt} (\bar{\Omega} \cdot \bar{\xi}_1)$$

Then

$$52) \quad \frac{dA_1}{dt} = - \frac{1}{(4\pi M_1)} \left( \frac{r_1^2}{9} \right) P_{1,2}$$

$$53) \quad \frac{dB_1}{dt} = A_1$$

When the mass shell bounding a central void collapses to the origin, then  $\ell = 1$  position perturbations,  $\xi_r$  and  $D$ , carry some average displacement which must then become the initial value of  $\bar{\xi}_1$  when the central mass point is formed. This average displacement is given by

$$54) \quad \bar{\xi}_1 = \frac{1}{4\pi} \int d\bar{\Omega}' \left[ \bar{\xi}_{r,1}(\bar{\Omega}') + \bar{\xi}_{\Omega,1}(\bar{\Omega}') \right]$$

and the scalar product,  $(\bar{\xi}_1 \cdot \bar{\Omega})$ , which is what we need for eqs. (51) through (53) is then,

$$55) \quad \bar{\xi}_1 \cdot \bar{\Omega} = \frac{1}{4\pi} \int d\bar{\Omega}' \left[ \bar{\xi}_{r,r} \cdot \bar{\Omega} + \bar{\xi}_{\Omega,1} \cdot \bar{\Omega} \right]$$

By definition of  $\xi_r(\bar{\Omega}')$ , where we have set  $\xi_{r,1}(\bar{\Omega}) = \xi_{r,1} Y_{1,m}(\bar{\Omega})$ ,

$$56) \quad \frac{1}{4\pi} \int d\bar{\Omega}' \bar{\xi}_{r,1}(\bar{\Omega}') \cdot \bar{\Omega} = \frac{\xi_{r,1}}{4\pi} \int d\bar{\Omega}' Y_{1,m}(\bar{\Omega}') \bar{\Omega}' \cdot \bar{\Omega}$$

for whatever  $m$  we are considering. The addition theorem, eq. (41), and orthonormality of the  $Y$ 's then give

$$57) \quad \frac{1}{4\pi} \int d\bar{\Omega}' \bar{\xi}_{r,1}(\bar{\Omega}') \cdot \bar{\Omega} = \frac{\xi_{r,1}}{4\pi} \int d\bar{\Omega}' Y_{1,m}(\bar{\Omega}') \left[ \frac{4\pi}{3} \sum_{m'=-1}^{+1} Y_{1,m'}^*(\bar{\Omega}') Y_{1,m}(\bar{\Omega}) \right]$$

$$= \frac{\xi_{r,1}}{3} Y_{1,m}(\bar{\Omega})$$

From the definitions in eq. (29) and the discussion above we have

$$58) \quad \bar{V}_{\Omega} \cdot \bar{\xi}_{\Omega,1} = D_1 Y_{1m}(\Omega)$$

Then from eq. (44) and (45)

$$59) \quad \frac{1}{4\pi} \int d\bar{\Omega} \bar{\xi}_{\Omega}(\bar{\Omega}) \cdot \bar{\Omega} = -\frac{D_1 r_1}{3} Y_{1m}(\Omega),$$

where  $r_1$  is the void boundary radius. Combining eqs. (55), (58) and (59) gives

$$60) \quad \bar{\xi}_1 \cdot \bar{\Omega} = \frac{1}{3} (\xi_{r,1} + r_1 D_1) Y_{1m}(\Omega)$$

which is the desired prescription for converting perturbations at  $r_1 > 0$  to a value of  $\bar{\xi}_1 \cdot \bar{\Omega}$  for a central mass point. This is done in the computations at a point when  $r_1 \ll r_2$ ,  $r_1$  is very near to 0, and the time step criterion for equations (32) and (33) is becoming prohibitive. At the same time  $D_l$  and  $C_l$  for  $l > 1$  are set to zero.

#### Artificial Viscosity

It is necessary to introduce a viscosity to accommodate shock waves even if the real physical viscosity is insignificant. Of the various possible forms of artificial viscosity, we have used only those which give a diagonal and isotropic stress tensor, i.e., a simple viscous pressure. In later treatments of real viscosity, however, off diagonal terms will be included together with a vector spherical harmonic treatment of perturbed quantities. While one dimensional codes, like an zero order spherically symmetric code, can and do sometimes use forms for artificial viscous pressure which are not proper scalars in the tensor sense, our need to generalize to more dimensions to include first order asymmetric contributions leads us to use only proper scalar forms. The forms we have used are

$$\begin{aligned}
61) \quad a) \quad P_v &= -\mu(\dot{\bar{V}} \cdot \bar{v}) \\
\quad b) \quad P_v &= -\mu(\dot{\bar{V}} \cdot \bar{v})^2 \\
\quad c) \quad P_v &= -\mu V^2 (\dot{\bar{V}} \cdot \bar{v}) .
\end{aligned}$$

In most uses these are turned on only when  $P_v > 0$  or when  $P_v (\dot{\bar{V}} \cdot \bar{v}) > 0$  to avoid negative viscous heating. Note that in an entropy based scheme even though there is no  $-PdV$  work term, where  $P$  is the pressure from the static equation of state, there is a  $-P_v dV$  work term which generates entropy. The values of  $\mu$ , which of course have different dimensions in different schemes, are computed locally to damp oscillations with a wavelength of the order the grid spacing on a time scale of about an acoustic period for this wavelength. Longer wavelengths are relatively much less damped. In practice we have usually used a combination of eqs. (61a) and (61b). The (61c) scheme has the advantage that it gives no artificial pressure in a region of uniform compression, and is used in cases where high compressions are obtained and values of  $\rho R$  that are obtained are sensitive to the form of  $P_v$ .

The differencing of  $P_v$ , both in zero and first order, is straightforward, if a bit tedious in some cases, and will not be reproduced here. The approach we have followed, which is in keeping with the integral, or finite element, approach of the rest of our model, is to try that  $(\dot{\bar{V}} \cdot \bar{v}) = \frac{1}{V} \frac{dV}{dt}$  for any cell volume.

It should be noted that when an on/off condition based on the sign of  $P_v$  or  $P_v (\dot{\bar{V}} \cdot \bar{v})$  is used in the zero order code, then the first order viscous pressure must also be switch on and off at the same times.

### First Order Heat Flow

The treatment of first order heat flow also proceeds by analogy with multidimensional Lagrangian methods. We generalize from the zero order equation (3). The heat flow through a zone boundary of area  $A$  across which there is a temperature difference  $\Delta T$  over a zone center separation distance of  $\Delta r$  is

$$(62) \quad F = \frac{-Ak\Delta T}{\Delta r}.$$

When all variables are written as a sum of zero and first order terms, the result is multiplied out, and zero and first order equations are separated, equation (62) becomes, in zero order,

$$(63) \quad F_0 = \frac{-A_0 \kappa_0 \Delta T_0}{\Delta r_0}$$

which when put in terms of radial indices is eq. 3 (above) and, in first order,

$$(64) \quad F_1 = \frac{-A_0 \kappa_0 \Delta T_0}{\Delta r_0} \left[ \frac{A_1}{A_0} + \frac{\kappa_1}{\kappa_0} + \frac{\Delta T_1}{\Delta T_0} - \frac{\Delta r_1}{\Delta r_0} \right].$$

In our system  $F_1$  has two parts, the radial part,  $F_{1r}$ , and the azimuthal part,  $\bar{F}_{1\Omega}$ , for which eq. (64) becomes continuous, and which will be treated as the variable  $\bar{V}_{\Omega} \bar{F}_{1\Omega}$ .

For  $F_{1r}$  we substitute into eq. (64) directly.  $T_1$  and  $\kappa_1$  are obtained at zone centers from equation of state information, and the  $\kappa$ 's are averaged to zone boundaries (see eq. (3)).  $\Delta r_{1j}$  is also chosen in a way that is consistent with eq. (3);

$$(65) \quad \Delta r_{1j} = \frac{(\xi_{r,j+1} + \xi_{r,j})}{2} - \frac{(\xi_{r,j} + \xi_{r,j-1})}{2} = \frac{-(\xi_{r,j+1} - \xi_{r,j-1})}{2}.$$

These substitutions into eq. (4) give, since  $A_{0,j} = r_j^2$ ,

$$66) \quad F_{1r} = \frac{-(\kappa_{o,j+1} + \kappa_{o,j})(T_{o,j+1} - T_{o,j})r_j^2}{(r_{j+1} - r_{j-1})/2} \times$$

$$\times \left[ \left( \frac{2\ell_{r,j}}{r_j} + D_j \right) + \left( \frac{\kappa_{j,j+1} + \kappa_{j,j}}{\kappa_{c,j+1} + \kappa_{o,j}} \right) + \left( \frac{T_{j,j+1} - T_{j,j}}{T_{o,j+1} - T_{o,j}} \right) - \left( \frac{\ell_{r,j+1} - \ell_{r,j-1}}{r_{j+1} - r_{j-1}} \right) \right]$$

where the first term in the [ ] brackets is  $\Lambda_{1,j}/\Lambda_{o,j}$ .

For  $\bar{F}_{1\Omega}$  eq. (64) simplifies because  $\Delta T_o$  is zero. Going to continuous dependence on  $\bar{\Omega}$  gives, where now  $\bar{F}_{1\Omega}$  is flux per unit area rather than flux per radian as in the case of  $F_r$ ,

$$67) \quad \bar{F}_{1\Omega,j} = \kappa_j \bar{V}_{\Omega} T_{1j}$$

or

$$68) \quad \bar{V}_{\Omega} \cdot \bar{F}_{1\Omega,j} = -\kappa_j V^2 \Omega T_{1j} = \frac{-4\ell(\ell+1)\kappa_j T_{1j}}{(r_{j+1} + r_j)^2}$$

Note that  $\bar{F}_{1\Omega,j}$  is defined in radius at the thermodynamic point, which we have taken to be  $(r_{j+1} + r_j)/2$ , (eq.3).

The desired result from the heat flow calculation is the rate of heat flow into a volume between zone boundaries which in the unperturbed state subtends a unit solid angle. We obtain for this rate,  $dQ_{F1}/dt$ , from a surface area integral of total flux over this volume

$$69) \quad \frac{dQ_F}{dt} = \frac{dQ_{Fo}}{dt} + \frac{dQ_{F1}}{dt} = \iiint d\bar{\Lambda}_{or} \cdot \bar{F}_{or} + \iiint d\bar{\Lambda}_o F_1 + \iiint d\Lambda_1 \cdot \bar{F}_o$$

The zero order terms reduce to the standard spherically symmetric form,

$$70) \quad \frac{dQ_{Fo,j}}{dt} = -(\Lambda_{oj} F_{or,j} - \Lambda_{o,j-1} F_{or,j-1}) = -(r_j^2 F_{or,j} - r_{j-1}^2 F_{or,j-1})$$

The first order terms are

$$71) \quad \frac{dQ_{F1}}{dt} = -\left( \iiint d\bar{\Lambda}_{\Omega} \cdot \bar{F}_{1\Omega} + \iiint d\bar{\Lambda}_{or} \cdot \bar{F}_{1r} + \iiint d\Lambda_{1r} \cdot \bar{F}_{or} \right)$$

where  $\Lambda_{r,j}$  is the area of the spherical end cap on the  $j^{\text{th}}$  mass surface and  $\Lambda_{\Omega,j}$  is the area of the sides of the zone (which disappear in the

continuous limit) between the  $j-1$  and  $j^{\text{th}}$  surfaces. The first term in eq. (71) we approximate as

$$72) \quad \oint \bar{\Delta}_{\Omega} \cdot \bar{F}_{1\Omega} = V_j (\bar{V}_{\Omega} \cdot \bar{F}_{1\Omega})_j - \frac{(r_j^3 - r_{j-1}^3)}{3} (\bar{V}_{\Omega} \cdot \bar{F}_{1\Omega})_j$$

by Gauss' theorem and assuming that  $(\bar{V}_{\Omega} \cdot \bar{F}_{1\Omega})_j$  is uniform over the volume  $V_j$ . The last two terms are treated as integrals over the end caps. Taking  $\Lambda_{1r}$  from eq. (12) and substituting eq. (72) along with the end cap terms gives

$$73) \quad \dot{Q}_{F_{1,j}} = \frac{dQ_{F_{1,j}}}{dt} - \frac{(r_j^3 - r_{j-1}^3)}{3} (\bar{V}_{\Omega} \cdot \bar{F}_{1\Omega})_j - (r_j^2 F_{1r,j} - r_{j-1}^2 F_{1r,j}) \\ - \left[ F_{or,j} r_j^2 \left( \frac{2\xi_{r,j}}{r_j} + D_j \right) - F_{or,j-1} r_{j-1}^2 \left( \frac{2\xi_{r,j-1}}{r_{j-1}} + D_{j-1} \right) \right].$$

Here we have used  $\Lambda_j = r_j^2$  and  $\frac{1}{\partial \bar{\Omega}} \frac{d}{dt} \equiv D_j$  (eq. 29) in eq. (12) for  $\Lambda_{1r}$ . Substituting for  $F_{or}$ ,  $F_{1r}$  and  $\bar{V}_{\Omega} \cdot \bar{F}_{1\Omega}$  from eqs. (3), (66), and (68) into eq. (73) gives the desired difference equation (which is too bulky to be worth writing out here).

#### Other Sources of Entropy

In addition to heat flow there are usually two other sources of entropy input to a zone in problems of interest, the viscous work,

$$74) \quad d\dot{Q}_v = -P \frac{dV}{vdt}$$

and laser or charged particle beam energy absorption,  $\dot{Q}_s$ , which is a source term usually given by trajectory integrals of an absorption co-efficient that may be a function of all state variables.

When eq. (74) is linearized it gives the standard zero-order equation and

$$75) \quad Q_{v_1} = - \left( \frac{P_{v_1}}{dt} \frac{dV}{v} + P_{v_0} \frac{dV}{dt} \right),$$

where, it will be recalled,  $V_j = (r_j^3 - r_{j-1}^3)/3$ . Both of these time

derivatives of volume also occur in the difference expression, for  $P_{v_0}$  and  $P_{v_1}$  as discussed below eq. (61).

In principle a wide variety of laser and charged particle beam energy absorption schemes are possible, so wide a variety that it would not be reasonable to try to present here a first order treatment of absorption that would be general enough to cover all of them. However, one prescription for laser energy absorption is so common that it will be discussed briefly here.

According to this prescription, to zero order light impinges on the spherical target along radial rays and is absorbed at that spherical surface on which the density,  $\rho$ , is equal to the critical density,  $\rho_c$ , (where the plasma frequency equals the laser frequency). The zone in which the energy is absorbed is then that zone whose density is in some sense closest to  $\rho_c$ . When first order corrections are considered it is clear that density perturbations do not change the mass surfaces between which the energy is deposited. That is, there are no first order corrections to the energy absorption rate,  $\dot{Q}_s$  in radially adjacent zones as there would be if the absorption were a much weaker function of density as it is in charged particle beam systems. However, the energy absorbed per unit mass in a zone increases or decreases as azimuthal perturbations increase, i.e., dilate; or decrease the surface area that the particular part of the surface of a zone presents to the incident rays. This correction, which is proportional to area perturbation is obtained from eq. (12) for  $\Delta_1$ .

There is a further first order correction to  $\dot{Q}_s$  the asymmetry of incident irradiation, which is naturally taken to be proportional



to  $Y_{j,1}$  and can be very important at low  $Z$  numbers. Combining the surface area and anisotropy perturbations gives

$$76) \quad Q_{S1,j} = Q_{S0,j} \left[ \frac{(d_j + d_{j-1})}{2} + q_{S1,j} \right]$$

where  $Q_{S0,j}$  is the zero<sup>th</sup> order source power in the  $j$  zone,  $q_{S1,j}$  is a constant first order relative anisotropy, and the  $d$ 's, which are defined on the mass surfaces and averaged to zone centers, are relative first order surface area dilatations given; from eq. (12) by

$$77) \quad d_{1j} = \left( \frac{2E_{r,i}}{r_j} + \frac{\partial \Omega_{1,i}}{\partial \dot{z}} \right) = \left( \frac{2B_i}{r_j} + D_j \right)$$

results. The perturbed energy from eqs. (73), (75) and (76) are now combined into a single term,

$$78) \quad \dot{Q}_{1,j} = Q_{1F,j} + Q_{1V,j} + Q_{1S,j}$$

which contains the first order corrections to all non-isentropic processes considered. Of course there is a parallel zero order equation for  $Q_{0,j}$ . We could now use tabular equation of state information or employ the following gamma law procedure.

First define a constant (arbitrary) reference value for the density,  $\rho_R$ , which is usually taken to be  $1(\text{gm/cm}^3)$  for convenience, and a corresponding quantity,  $P_{R,j}$ , with the dimensions of pressure, which is the pressure in the  $j^{\text{th}}$  zone when  $\rho_j = \rho_R$ , and which is a function of time as well as space in non-isentropic situation.

Then the gamma law equation of state is

$$79) \quad P_j = P_{R,j} \left( \frac{\rho_j}{\rho_R} \right)^\gamma$$

It will be recalled that the constant  $\gamma$  is  $5/3$  for a fully ionized plasma or monatomic gas,  $7/5$  for a diatomic gas, and  $1$  for any

isothermal fluid. For the gamma law the internal energy for the  $j^{\text{th}}$  zone is

$$80) \quad E_j = \frac{V_j n_j k T_j}{(\gamma-1)} = \frac{(r_j^3 - r_{j-1}^3) \rho_j (1+Z)}{3(\gamma-1) m_i} \times k T_j \frac{M_i (1+Z) k T_j}{3(\gamma-1) m_j}$$

where  $M_j$  is the (thermodynamic) mass of the zone,  $k$  is the Boltzmann constant,  $m_i$  is the mean ion mass,  $Z$  the mean ionization state, and  $n_j$  is the mean particle density. Also, of course, independent of  $\gamma$ ,

$$81) \quad P_j = n_j k T_j = \frac{\rho_j (1+Z)}{m_i} k T_j$$

To calculate perturbed pressures we linearize eq. (79), by assuming  $P_{R,j} = P_{RO,j} + P_{R1,j}$ , differentiate with respect to time and obtain, with the help of eq. (80) and (81),

$$82) \quad \frac{dP_{RO,j}}{dt} = \frac{(\gamma-1) \dot{Q}_{o,j}}{(\rho_{o,j}/\rho_R)^\gamma v_j}$$

$$83) \quad \frac{dP_{R1,j}}{dt} = \frac{(\gamma-1) \left[ \dot{Q}_{1,j} - \dot{Q}_{o,j} \left( \frac{\rho_{1,j}}{\rho_{o,j}} \right)^\gamma (\gamma-1) \right]}{v_j (\rho_{o,j}/\rho_R)^\gamma}$$

and the zero and first order temperatures are

$$84) \quad T_{o,j} = \frac{P_{RO,j} \left( \frac{\rho_{o,j}}{\rho_R} \right)^\gamma}{n_{o,j} k} = \frac{P_{RO,j} m_j}{(1+Z) k \rho_R} \left( \frac{\rho_{o,j}}{\rho_R} \right)^{(\gamma-1)}$$

$$85) \quad T_{1,j} = \left[ \frac{P_{R1,j}}{P_{RO,j}} + (\gamma-1) \left( \frac{\rho_{1,j}}{\rho_{o,j}} \right)^\gamma \right] T_{o,j}$$

This equation of state procedure or its tabular equivalent for less idealized material properties, is in fact entropy based. It avoids calculating the hydrodynamic work and the accumulation of truncation errors in that usually large term. In general it has the advantages of any numerical scheme which treats physically conserved,

(or nearly or sometimes conserved), quantities (here specific entropy) in such a way that when they should be constant they are really constant to round off.

### III. THE PARTICLE LAGRANGEAN (PAL) METHOD

For studying aspects of implosions which are too distorted to permit a perturbation treatment, and in particular for studying the non-linear saturation of the Rayleigh-Taylor instability discussed in Section II and Refs. 1, 2 and 5, a Particle-In-Cell type method has been developed which is more Lagrangean than the original PIC method (Ref. 3). This method we call PAL for Particle Lagrangean. The PAL method has been incorporated in a two dimensional, cylindrically symmetric code called IRIS with a fixed rectangular grid in  $r$  and  $z$  and regular grid, i.e., cell, intervals ( $\Delta r$ ,  $\Delta z$ ). Recall that PIC (Ref. 3) defines the different hydrodynamic variables on the fixed grid the way the pure Eulerian method does but also associates the mass with fixed mass particles. The particle masses are, however, in general not all the same. The particles are moved with a velocity which is interpolated to the particle positions from the cell centers. The cell center velocity is obtained by dividing cell momentum by mass. The mass in a cell (or zone) at a given time is then obtained by adding the masses of the particles in the cell at that time. Momentum and energy are transported between adjacent cells during a given time step in proportion to the fraction of cell mass crossing cell boundaries with the particles.

The PAL method associates momentum and an internal thermodynamic variable, such as the specific entropy used in IRIS, in addition to mass, with the particles. In this respect the method resembles the "collisionless" PIC method developed for plasma simulation purposes (Ref. 6). However, unlike nearly collisionless plasmas with their distribution of particle velocities at any point,

fluids have a velocity field which is a single valued function of position. Therefore, cell center momenta and velocities are obtained by summing particle momenta, and the particles are moved according to interpolated values of these cell velocities as in standard fluid P.I.C. Cell center accelerations are calculated from a sum of forces on cell faces and from cell mass, and particle momenta are incremented during a time step by an interpolated distributing of the corresponding cell momentum change over the particles in a cell in proportion to their mass. In summary, the quantities defined on cell centers and on particles are given in the following lists. Note duplication of those quantities which are summed or interpolated between cells and particles.

Particle Quantities: Mass,  $m$ ; momentum or velocity,  $\vec{v}$  or  $\vec{p}$ ; specific entropy,  $s$ .

Cell Quantities: Mass,  $M$ ; momentum or velocity,  $\vec{P}$  or  $\vec{V}$ ; entropy,  $S$ ; temperature and pressure,  $T$  and  $P$ ; acceleration,  $a$ .

It is clearly possible for individual particle velocities to accumulate large departures from the local average cell velocities.

This has been limited in practice by applying a small rate of damping (i.e., smoothing) of particle velocities toward the local cell velocity in a momentum conserving way. Happily, it has not been found necessary to use damping rates that significantly modify computed flows. The time stepping procedure used calculates all quantities at half and whole time steps in a way that is similar to two step Lax Wendroff (Ref. 7) and gives second order accuracy in the time step,  $\Delta t$ . This procedure requires two passes through the particle table for a given time step, but this expense is more than compensated for by the second order accuracy in  $\Delta t$ . Special care

has been taken in prescribing the details of the calculation of forces on vacuum interfaces, i.e., free-surfaces, to conserve momentum and to avoid the spurious heating and acceleration of cells in such interface regions, which is sometimes obtained by PIC methods.

Heat flow, which in our physical applications is by electron thermal conduction (Ref. 8), is treated implicitly in time for the reason that the thermal conductivity is a strong function of temperature and in some parts of most problems becomes very large. These large conductivities would require an unacceptably small value of  $\Delta t$  to obtain stable forward differenced solutions of the heat flow equation (Ref. 9). There are several ways that the implicit formulation of the two dimensional heat flow equation can be solved. The method we have used is called splitting (Ref. 10). This method, which is particularly well suited to regular cell grids, effectively decomposes a two dimensional calculation into two sets of orthogonal one dimensional calculations which are easily done by standard 1d implicit methods. Second order accuracy in  $\Delta t$  is obtained by performing two sets of  $r$  and  $z$  1d calculations on each time step (see Ref. 10).

Fig. 1 illustrates the way the IRIS code has been used to study the problem of non-linear development of Rayleigh-Taylor instability in imploding spherical shells. The sketch on the left shows a conical section of the shell in its initial position (dashed lines) and at some intermediate time in the implosion process. We take the view that up to this time the initial perturbations on the unstable outside surface have grown from small amplitudes to amplitudes of the order of the perturbed mode wavelength on the surface and that during this early period unstable growth is correctly described by

the linearized treatment (above). However, when the unstable mode amplitude becomes of the order of the wavelength, a full multi-dimensional calculation is required to treat the subsequent shell breakup or other non-linear saturation processes that may occur. For this purpose the center axis of the cylindrical grid of the code is placed on a radius of the spherical system, as indicated in Fig. 2, and in this way a small pill-shaped section of the imploding shell is simulated. The outside surface of the grid is rigid but allows free tangential slip, and the ends are rigid. Since in general the most unstable shell distortions pass from moderate non-linearity (amplitude slightly less than wavelength) to shell breakup or saturation as the shell moves only a few times its length. Consequently, as will be seen below, when the shell thickness is much less than its spherical radius, the grid need not be extended so near the origin (i.e., so far in  $x$ ) that its cylindrical shape is seriously in conflict with the spherical geometry of the Laplace system.

Two opposite sample cases are shown here. In the first, indicated in the upper right of Fig. 2, the shell is pushed inward by the pressure of a lower density, and usually lower atomic number,  $Z$ , outer layer (region 2) of blowoff material (Ref. 1) which is a much better thermal conductor than the higher density inner shell, which in this case is SiO<sub>2</sub> ( $Z = 10$ ), a favorite laser fusion shell material, and is heated and raised to a high pressure from the outside by the laser or charged particle beam. There is, however, no thermal conduction in the calculation corresponding to the fact that conduction and ablation are not important in this type of explosion. The interface, which is unstable under these conditions, is perturbed with an amplitude  $1/3$  of its wavelength. A code with wavelength

about equal to shell thickness was chosen because the combination of higher growth rates at shorter wavelengths and greater ability to break up the shell when the wavelength is longer is generally believed to make this the most dangerous mode. The initial  $\text{SiO}_2$  shell density is  $2 \text{ gm/cm}^3$  and that of the lower density plastic blow off layer  $2/3 \text{ gm/cm}^3$ . For these calculations a regular square grid of 36 (in  $r$ ) by 170 (in  $z$ ) zones and 132,110 particles were used. The lower right sketch in Fig. 2 illustrates the second case, which is the same in other respects but has the lower density blow off layer removed and its effect replaced by the pressure of direct ablation from the  $\text{SiO}_2$  shell. The incident laser light is deposited at critical density (laser frequency equals plasma frequency) of  $0.2 \text{ gm/cm}^3$ . Thermal conduction is important and is included here; incident laser power is  $10^{14} \text{ W/cm}^2$  and temperatures of about 2 keV are reached in the ablated material. Ablated material reaching the ends of the grid is allowed to flow out freely. To compensate for the removal of shell material by ablation the shell material was made initially twice as thick, which is 2.5  $\mu$  in this case, and the perturbation amplitude correspondingly twice as large.

Figs. 3a and b show time sequences of density contours from the blow off layer and ablative driven cases respectively. An important difference is readily seen. The shell that is driven by the pressure of lower density material without thermal conduction (3a), which is essentially the classical Rayleigh-Taylor unstable situation, shows the instability continue to grow past the small amplitude level and break up the shell into isolated regions of moderate density. The lower density blow off layer material squirrels between these higher density regions toward the center of the spherical implosion system as can be seen in plots of the flow velocity field



(not shown). This type of behavior would constitute extreme disruption of the implosion and would preclude achieving the high compression of fuel inside of the shell which inertial confinement fusion requires for economical performance.

The ablative driven case, Fig. 3b, shows seemingly much more stable behavior in spite of the fact that small amplitude calculations with the small amplitude method of Section II above find instability growth rates for this case with thermal conduction and the above blow off driven case without conduction very nearly the same. Notice that in spite of some persistent ripples on the outside of the shell, the higher density middle of the shell is essentially laminar, in contrast with the isolated regions of higher density seen above. This laminar form would produce the type of essentially spherically symmetric implosion desired. What has been encountered in these two dimensional simulations of ablation is apparently a non-linear saturation mechanism which is caused by lateral (parallel to the surface) heat flow in the ablation region. This conjecture about lateral heat flow is prompted by detailed examination of the results, which show this. Evidently this effect could be very important for laser fusion. If so, the ablative system would be much better than that driven by a blow off layer. However, in the particular case shown here the ablation rate is on the high end of the range of interest. More than the few runs which have been made so far will be needed to map out the ranges of physical parameters in which this non-linear ablative stabilization can be expected to occur.

## REFERENCES

1. Fraley, Gela, Henderson, McCrory, Milone, Mason & Morse, Plasma Physics and Controlled Nuclear Fusion Research, (International Atomic Energy Agency, Vienna, 1974), Paper IAEA-CN-33/F5-5.
2. "Stability & Symmetry of Laser Driven Implosions, I Solid Spheres, II Spherical Shells," R. L. McCrory & R. L. Morse, to be published.
3. Harlow, F. H. (1964). In "Meth. In Comp. Phys." 3, 319. Academic Press, New York.
4. R. D. Richtmyer & K. W. Morton (1967). "Difference Methods For Initial Value Problems," (2nd ed.) p. 293ff, Interscience, NY
5. D. B. Henderson & R. L. Morse, Phys. Rev. Letter 32, 355 (1973); J. N. Shiau, E. B. Goldman & C. I. Wong, Phys. Rev. Letter 32, 352 (1973); D. B. Henderson, R. L. McCrory and R. L. Morse, Phys. Rev. Letter 33, 205 (1974).
6. Morse, R. L. (1970) in "Meth. In Comp. Phys." 9, 213 Academic Press, New York.
7. Ref. 4, p. 300ff.
8. I. Spitzer (1956), "Physics of Fully Ionized Gases," p89ff, Interscience, New York.
9. Ref. 4, p. 9ff.
10. Ref. 4, p. 216ff.
11. Chandrasekhar, S., (1961), "Hydrodynamics & Hydromagnetic Instability," Ch.X, Clarendon Press, Oxford.

Fig. 1 These diagrams illustrate the way the linearized perturbation difference equations are derived by taking the limit of multidimensional Lagrangean difference equations as the difference intervals in angle about the spherical center go to zero and the angular variation becomes continuous. (1a) Illustrates the limiting process in which the angular dimensions of zones vanish while radial intervals remain finite. (1b) Shows the origin of the angular forces  ${}^1\bar{f}_{\Omega_1,j}$  and  ${}^2\bar{f}_{\Omega_1,j}$  from departures from spherical symmetry and from angular differences of pressures applied to radial pannels respectively. This sketch shows the discrete angular interval situation before the continuous limit is taken. (1c) Shows the geometry of the radial pannels on which angular pressure differences act. (1d) Shows the geometry of the particular treatment that must be given to the mass point at the spherical center when treating  $m = 1$  perturbations.

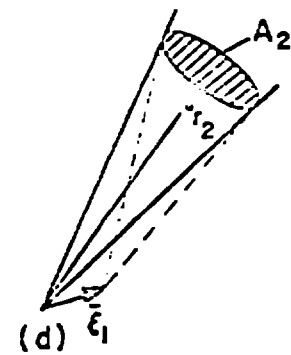
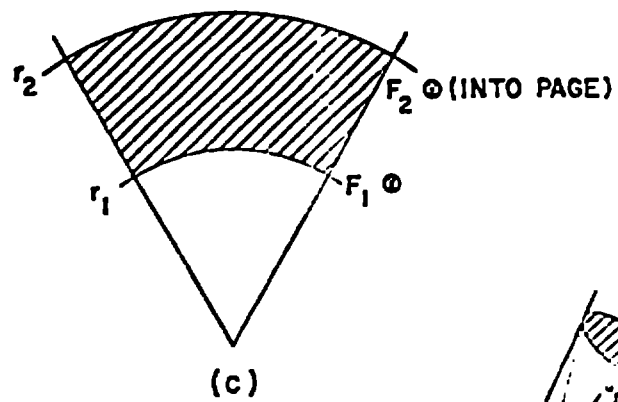
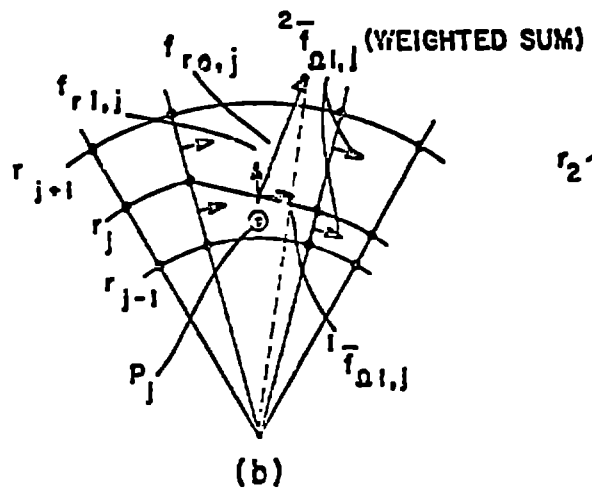
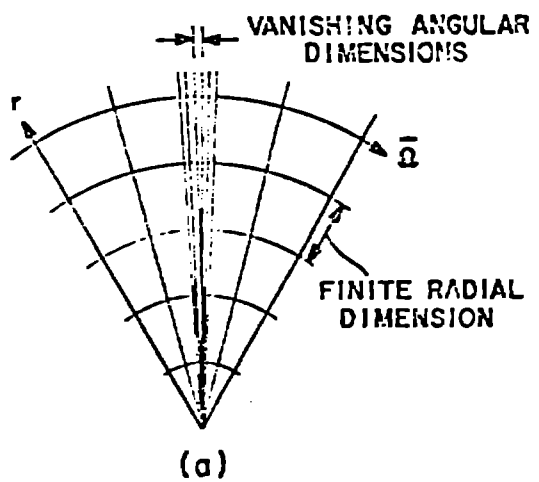


Fig. 2 The schematic arrangement of the cylindrical grid of the PAL code to treat a circular section of an imploding shell is shown on the left. On the right are shown the initial conditions for the two different modes of driving the shell to implode. The upper figure shows the initial conditions for the mode in which a lower density outer fluid at higher pressure pushes the higher density shell. In this case there is no heat flow. The lower figure shows initial conditions for a case run with electron thermal conduction in which ablation pressure caused by absorbed laser light energy drives the implosion.

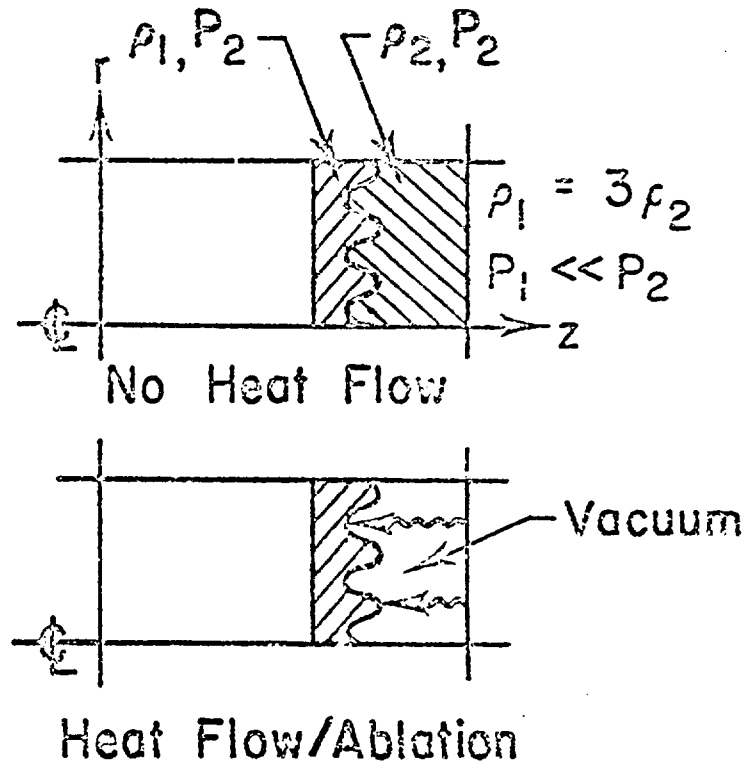
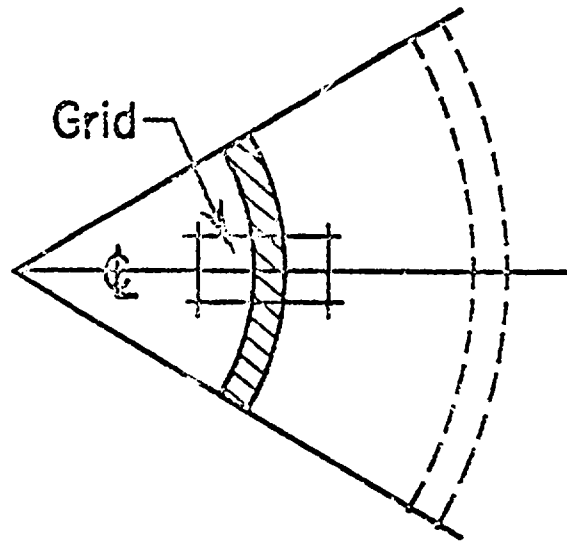
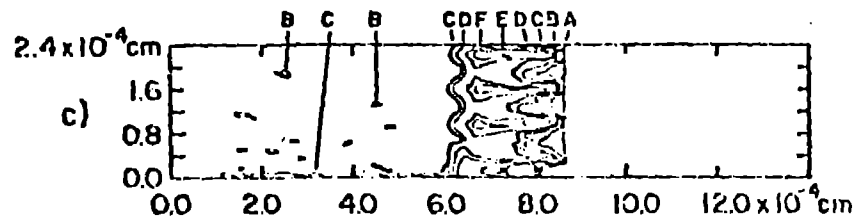
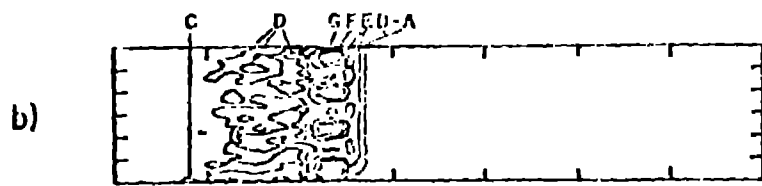
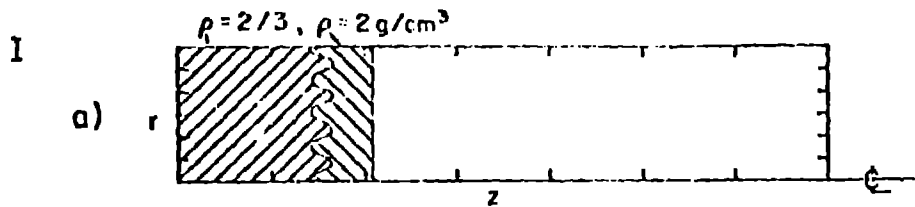
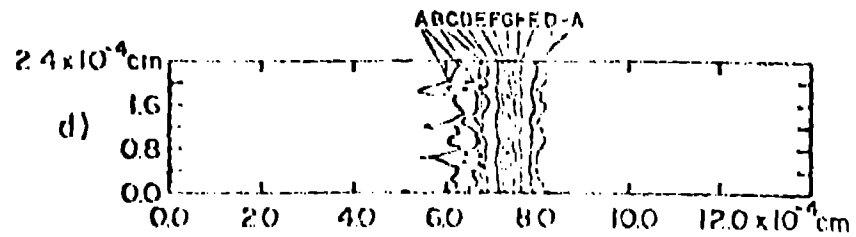
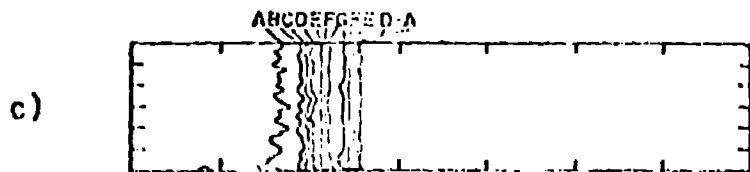
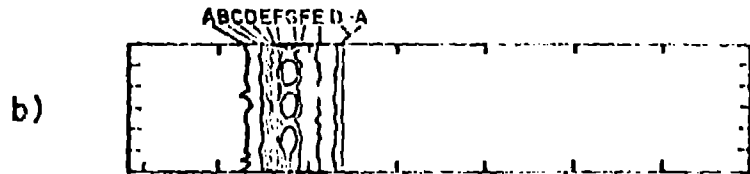
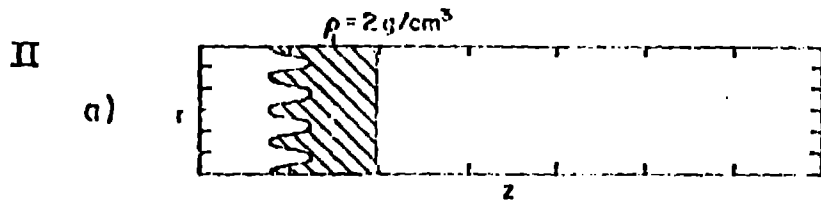


Fig. 3      Contours of density illustrating results of the two cases whose initial conditions are shown schematically in fig. 2. Case I is the case without heat flow. Case II is the laser driven ablative case. Note that the direction of motion in  $Z$  has been reversed from that shown in fig. 2, ie., motion is to the right in both cases here and the laser is incident from the left in Case II. In both cases the first frame shows initial conditions and subsequent frames going down show the isodensity contours at later times. Note the sharp contrast between case I in which the shell is broken into clearly isolated regions of relatively high density and the ablative case II in which the flow is almost laminar and the shell integrity is essentially preserved.



CONTOUR VALUE

A - 4.603E-03 g/cm<sup>3</sup>  
 B - 1.644E-01  
 C - 2.843E-01  
 D - 4.041E-01  
 E - 1.603E+00  
 F - 2.801E+00  
 G - 4.000E+00





### **Acknowledgment**

**This work was supported by the United States Energy Research and Development Agency.**